Supplementary material

BH3-only proteins are part of a regulatory network that control the sustained signaling of the Unfolded Protein Response sensor IRE1α

Diego A. Rodriguez et al. 2012

Supplementary Figure legends

Figure S1. Distinct BH3-only proteins co-immunoprecipitate with IRE1α. (**A**) HEK293 cells were co-transfected with an expression vector for a VSV-tagged version of the cytosolic domain of IRE1α (IRE1ΔN-VSV) together with expression vectors for indicated HA tagged BH3-only proteins or empty vector (Mock). As positive control, a PUMA-HA construct was employed. In addition, non-transfected (NT) cells were employed as control. After 48 h, protein extracts were prepared in CHAPS buffer (see methods) and HA immunoprecipitated with anti-HA antibody-agarose complexes. Protein complexes were eluted by competing with an excess of HA peptide and co-immunoprecipitation assessed by Western blot analysis. Red arrowheads indicates the band corresponding to each BH3-only protein expressed. (**B**) BAX and BAK DKO cells were reconstituted with an AU1-BAK-cb5 expression vector or mock, and then cells were transduced with retroviruses expressing HA-BIM-cb5 or empty vector (Mock) in the presence of 7.5 μM zVAD-fmk to prevent cell death. Then, transduced cells were treated or not with 100 ng/ml Tm for 16 h. Upper panel: HA was immunoprecipitated using anti-HA antibodies conjugated to protein G-sepharose. Co-immunoprecipitation of IRE1α was detected by Western blot. Lower panel: Expression of indicated protein in the cell lines is presented using Western blot with anti-HA and anti-AU1 antibodies, respectively. Tubulin was used as loading control. (**C**) BNip3 expression was analyzed by Western blot in WT or BIM

and PUMA DKO cells at basal level or after the treatment with Tm (100 ng/mL) for 16 and 24 h. Mouse brain protein extracts from cortex was used as positive control. The amount of total protein used was 50 μg for MEFs and increasing amounts for brain tissue (12.5, 25 and 50 μg). HSP90 was used as loading control.

Figure S2. BIM and PUMA double deficiency decreased XBP-1 mRNA splicing, XBP-1s-dependent target transcription and cell death. (**A**) Raw data of quantification of Figure 2B. WT (White dots) and BIM/PUMA DKO (Black dots) cells were treated for indicated time points with Tm (100 ng/mL). XBP-1 mRNA splicing was monitored by RT-PCR. PCR fragments corresponding to the unspliced (XBP-1u) or spliced (XBP-1s) forms of XBP-1 mRNA were quantified by densitometric analysis. The amount of unspliced + spliced XBP1 was counted as 100% splicing for each time point. Graph shows the percentage of the spliced form (XBP-1s, %) for individual time points of three to five independent experiments. The average of all point is indicated as single line for WT and dot lines for DKO MEFs cells. **(B**) WT and BIM/PUMA DKO cells were incubated in presence of 1.25 mM DTT for 16 and 24 h. Then XBP-1 mRNA splicing was monitored by RT-PCR. (**C**) WT and BIM and PUMA DKO cells were incubated for indicated time points with a high dose of Tm (1.0 μg/mL). XBP-1mRNA splicing was monitored by RT-PCR. (**D**) The expression *of bip*, and *chop* mRNA was monitored in WT and BIM/PUMA DKO cells treated with Tm (100 ng/mL) for 4 and 8 h by real time PCR. Actin expression was assessed as housekeeping gene. All data sets represent three independent experiments (mean and standard error). Statistically significance was calculated with multiple comparisons using ANOVA (Newman-Keuls Multiple Comparison Test, *: $p < 0.05$, n.s. non significant). (**E**) WT and BIM/PUMA DKO cells were treated with 100 ng/ml Tm or 500 nM Thap for indicated time points. Then, cell death was quantified by propidium iodide staining and FACS analysis. In all experiments, mean and standard

deviation is presented. (**F**) Upper panel: WT and BIM/PUMA DKO cells were incubated with high doses of Tm (3 μg/mL) for 5 h. Then, *blos1* and *col6* mRNA levels were quantified by real time PCR. *rpl19* was used as a housekeeping gene. Data from three independent experiments is expressed as log2 of the ratio of Tm-treated versus untreated cells. Lower panel*:* for all conditions XBP-1 mRNA splicing was monitored by RT-PCR.

Figure S3. Control experiments to test the effects of BIM and PUMA double deficiency on XBP-1 mRNA splicing. (**A**) To monitor the activity or stability of Tm and Thap in the kinetic studies, IRE1α KO and reconstituted cells with an IRE1a-HA construct were treated with 100 ng/ml Tm or 100 nM Thap for indicated time points (upper panel). Then, the cell culture media for each time point was collected and used to treat new cells for additional 6 h (bottom panel). Then in all conditions XBP-1 mRNA splicing was monitored by RT-PCR. (**B**) ER stress does not alter the stability of *xbp-1* mRNA. WT and BIM/PUMA DKO cells were treated with 1.0 mg/mL of Tm for 3 h to trigger complete XBP-1 mRNA splicing. Then, transcription was block by a treatment with 3 mg/mL actinomycin D and the decay of *xbp-1* mRNA was followed over time by semi-quantitative RT-PCR in total cDNA. Data were normalized with the XBP-1 mRNA levels from control cells not treated with actinomycin D. Right panel: Densitometric analysis of experiments presented in the gels. Data is expressed as percentages respect to WT or DKO cells without treatment.

Figure S4. Decreased IRE1α oligomerization and JNK phosphorylation in BIM and PUMA DKO cells. (**A**) WT and BIM/PUMA DKO cells were treated with 100 ng/ml for the indicated time points. Then IRE1α multimers were visualized using non-denaturating

polyacrylamide gels (absence of SDS in samples). To analyze total levels of IRE1α as monomers, the same samples were monitored using SDS-denaturating gels. HSP90 levels were monitored as loading control. (**B**) The expression pattern of IRE1α was visualized in WT and BIM/PUMA DKO cells under basal conditions. Cells were analyzed by indirect immunofluorescence and confocal microscopy. Cellular localization of IRE1α (green) and an ER marker (anti-KDEL staining, red) are shown. Scale bar: 10 μM. Merged images were generated including Hoechst staining (nucleus, blue) using the Image J software program. (**C**) WT and DKO cells were incubated as in B and the levels on JNK phosphorylation, total JNK, and HSP90 were monitored using Western blot analysis. Data is representative of three independent experiments.

Figure S5. No effects of BIM and PUMA double deficiency on ER calcium homeostasis. (**A**) BIM and PUMA WT and DKO cells were loaded with the calcium indicator Fura-2 and then stimulated with 10 μM ionomycin (Iono, left panel) or 5 μM thapsigargin (Thap, right panel) in the absence of extracellular calcium. Then, cytosolic calcium signals were monitored with a confocal microscope over time. The maximum calcium signal from was quantified in a total of three independent experiments is also presented in he graph bars, normalized with the values obtained in WT cells. Arrows indicate time of addition of the calcium agonist. (**B**) For comparison, similar experiments were performed in BAX/BAK WT and DKO cells. In A and B, mean and standard error are shown. Statistically significant differences detected with Student-T Test; *: $p < 0.01$; **: $p < 0.001$; ns: non significant.

Figure S6. Effects of ABT-737 on XBP1 mRNA spicing, and control experiments. (**A**) WT MEFs cells were pre-treated with 5 μM z-VAD-fmk for 30 min and then treated with

100 ng/ml of Tm in absence or presence of ABT-737 (1 μM). At indicated time points, levels of XBP-1 mRNA splicing were monitored by RT-PCR. (**B**) The expression levels of XBP-1s were monitored by immunoblot in cells treated with the indicated Tm concentration for 8 h in the presence or absence of 1 μM ABT-737. Nuclear extracts were employed, and SP1 levels were monitored as loading control. (**C**) Synthesis of BIM and PUMA by IVTT was assessed by radio-labeling and determined by electrophoresis and autoradiograph analyzing 5 ml of the IVTT product. Middle panel: 20 μg of recombinant IRE1ΔN were separated by protein electrophoresis, then transferred into a membrane and stained with ponceau red. As control a molecular weigh standard was used (Std). Right panel: 100 ng of recombinant BCL-2 was analyzed by Western blot using an anti-BCL-2 antibody. Proteins of the expected molecular weight are indicated with an arrowhead.

Figure S7. The BH3-only protein BAD modulates XBP-1 mRNA splicing and immunoglobulin secretion of LPS-stimulated B cells. (**A**) Primary B cells were purified from spleens of bad-/- and bad+/+ mice. Then, the cells were stimulated with LPS (0.1, 1.0 and 10 μg/mL). After 2 days of culture, IgM concentrations measured in the supernatant by ELISA. (**B**) In the same experiments, XBP-1 mRNA splicing was monitored by RT-PCR. (**C**) A summary of the function of different BCL-2 family members in apoptosis pathway and the specific role in UPR is presented based on this study and previous literature. &: Activator BH3-only proteins, #: sensitizer BH3-only proteins.

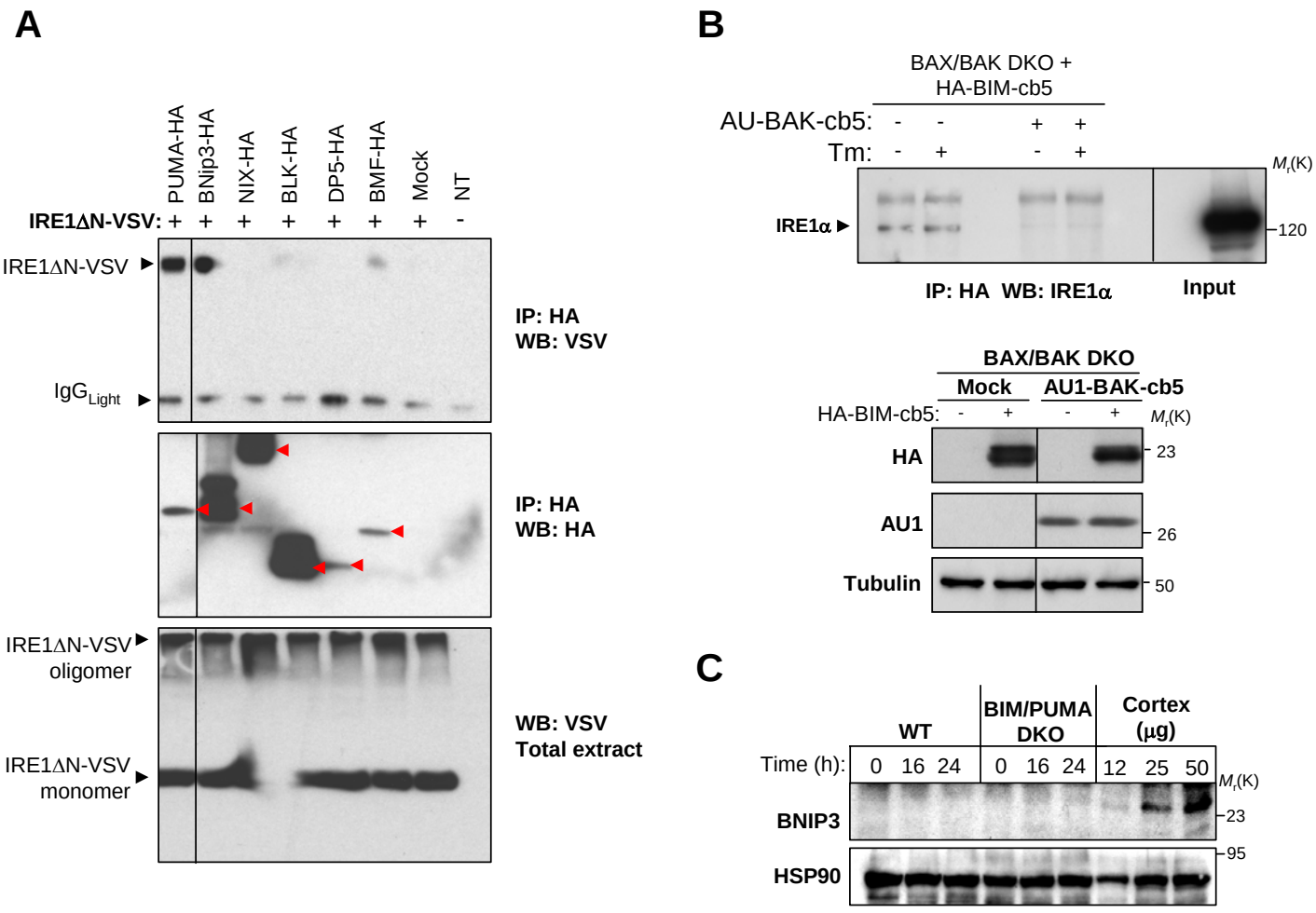

Supplementary Fig. 1

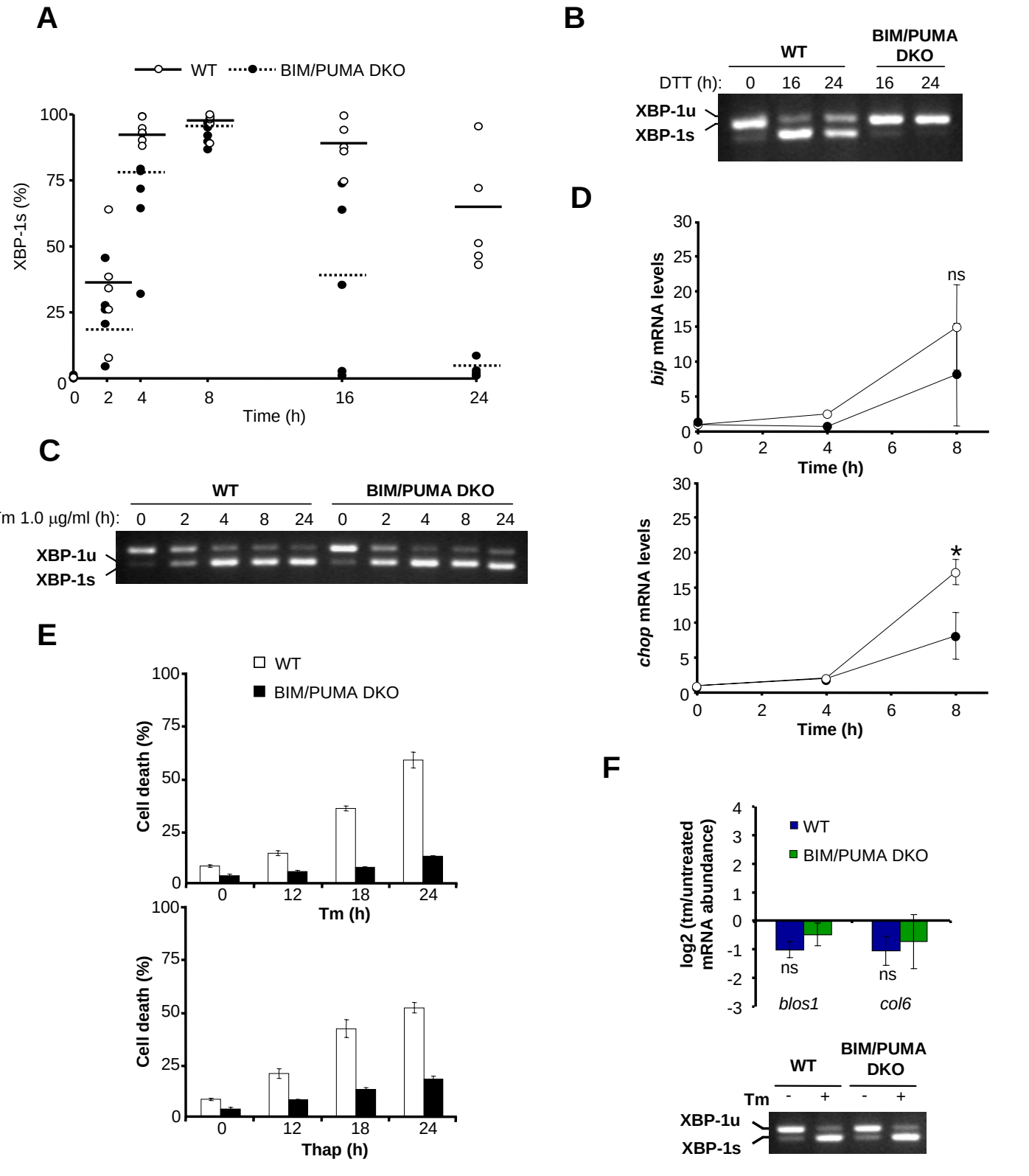

Supplementary Fig. 2

A

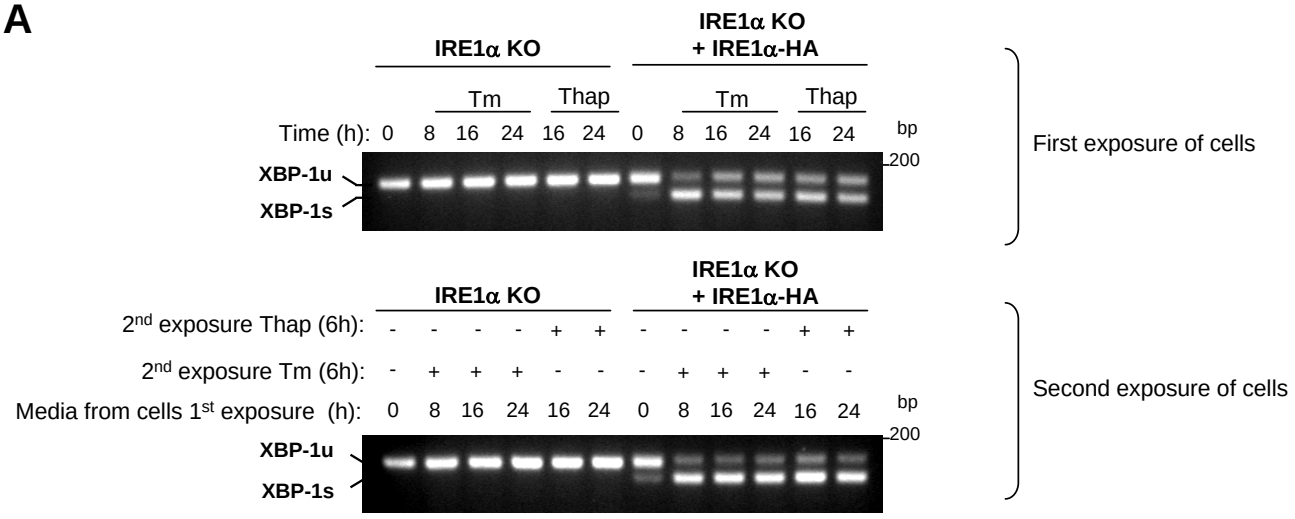

B

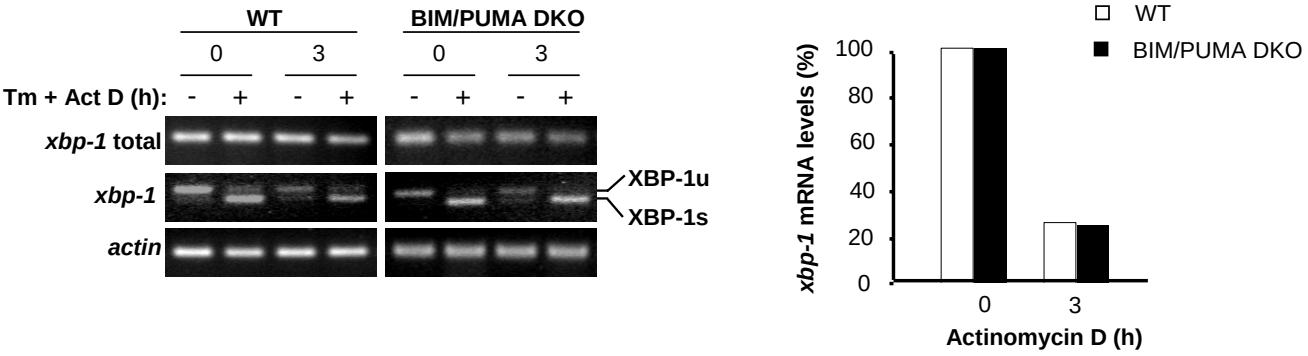

Supplementary Fig. 3

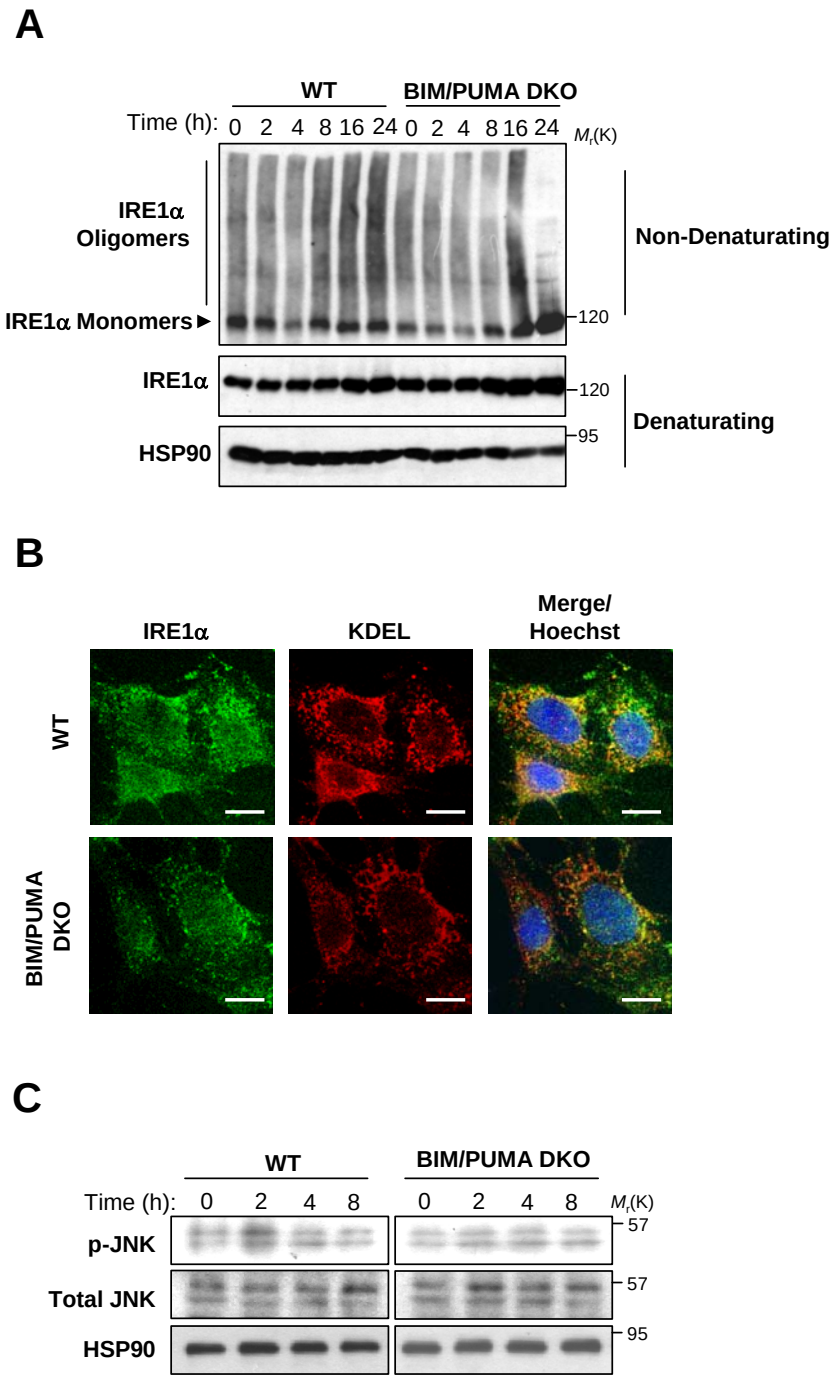

Supplementary Fig. 4

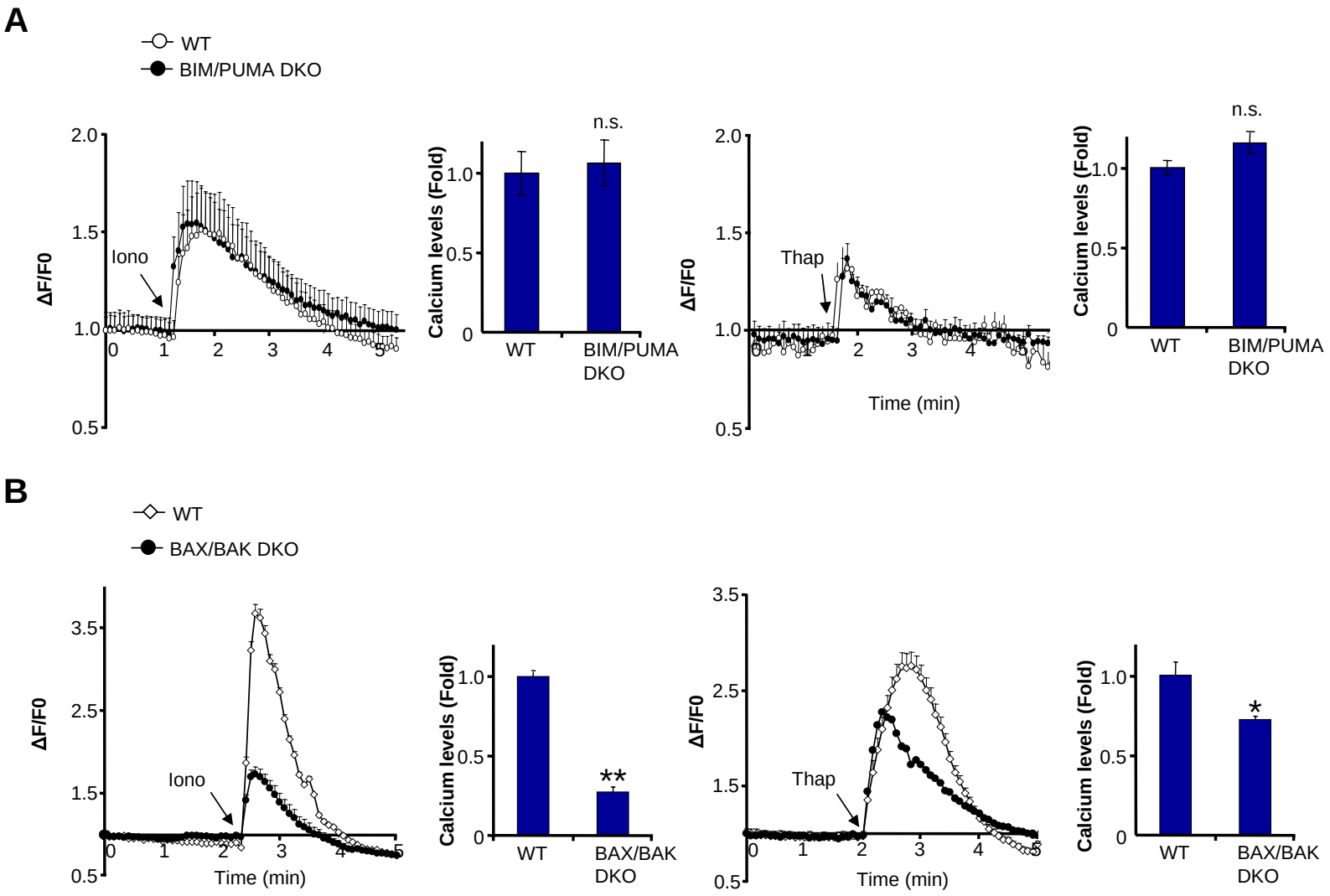

Supplementary Fig. 5

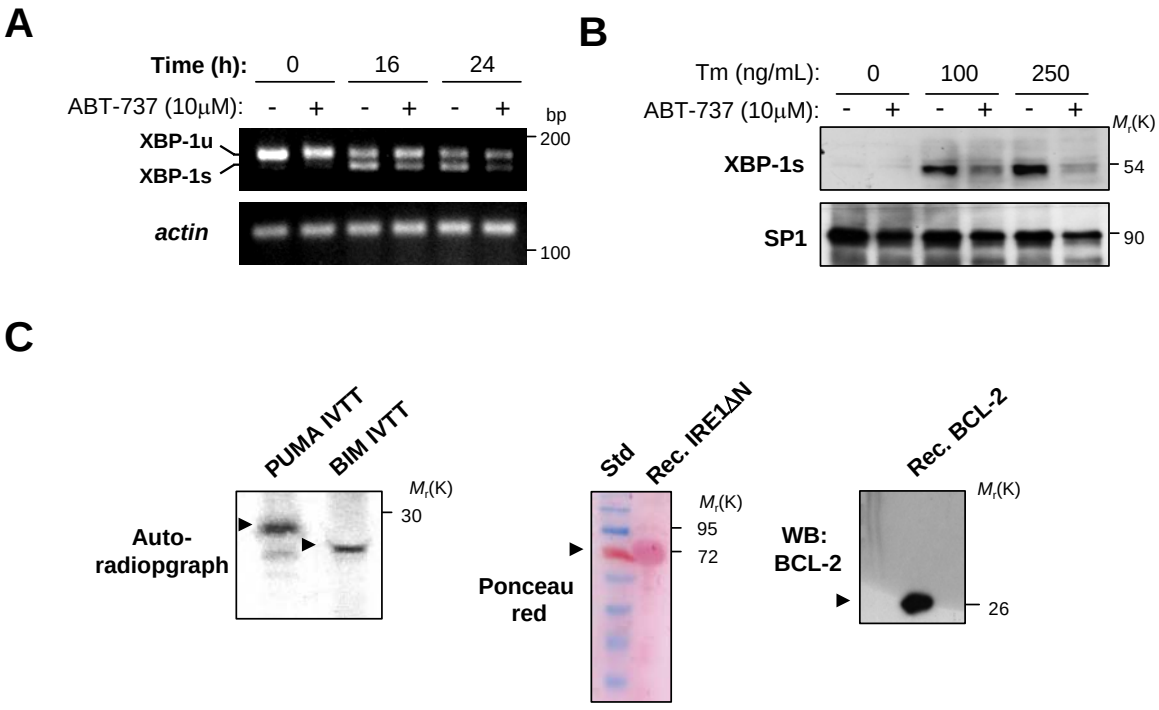

Supplementary Fig. 6

A

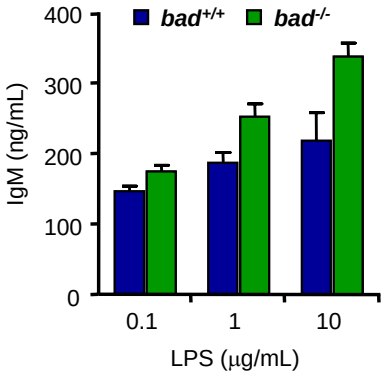

B

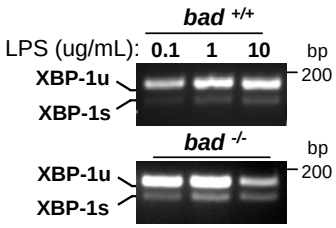

C

BCL-2 family member	Cell death activity	IRE1α regulation
BIM	Pro-apoptotic &	Activator
PUMA	Pro-apoptotic &	Activator
BID	Pro-apoptotic &	Non
BAD	Pro-apoptotic #	Inhibitor
NOXA	Pro-apoptotic #	Non
BAX	Pro-apoptotic	Activator
BAK	Pro-apoptotic	Activator
BCL-2	Anti-apoptotic	Activator
BCL-X_L	Anti-apoptotic	Non
MCL-1	Anti-apoptotic	Non

&, activator BH3-only;
#, Senzitizer

Supplementary Fig. 7